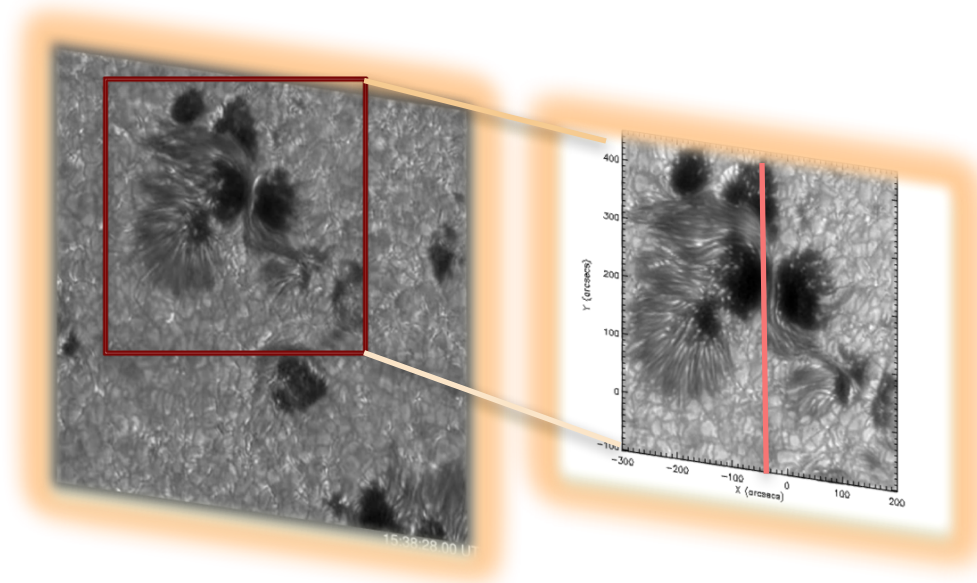


Continuum emission enhancements in flares observed by ROSA and IRIS



*F. Zuccarello, V. Capparelli, M. Mathioudakis,
P. Keys, L. Fletcher, S. Criscuoli, M. Falco,
S.G. Guglielmino, M. Murabito*

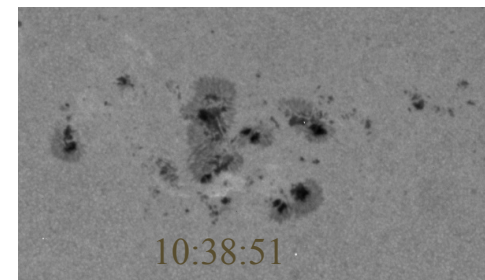
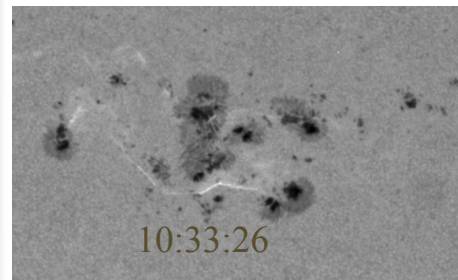
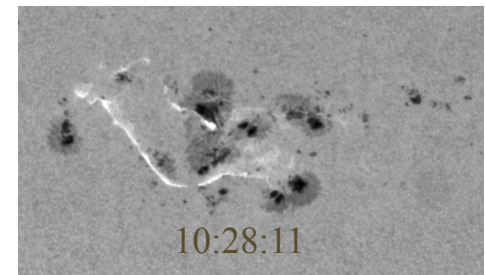
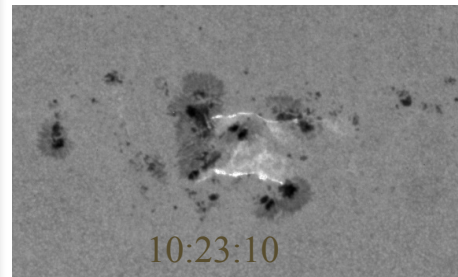
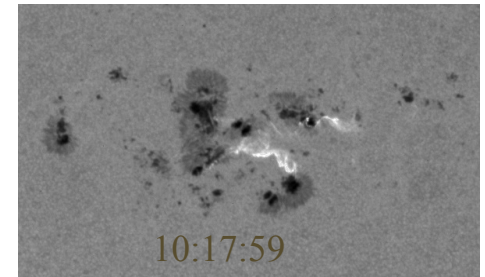
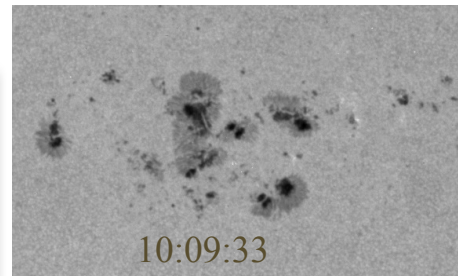
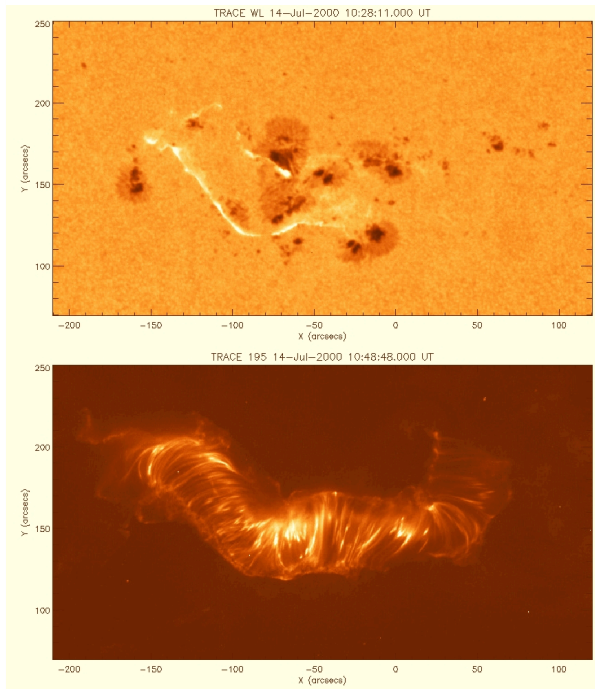


e-poster

*EST Science Meeting
June 11-15, 2018
Giardini-Naxos, Italy*

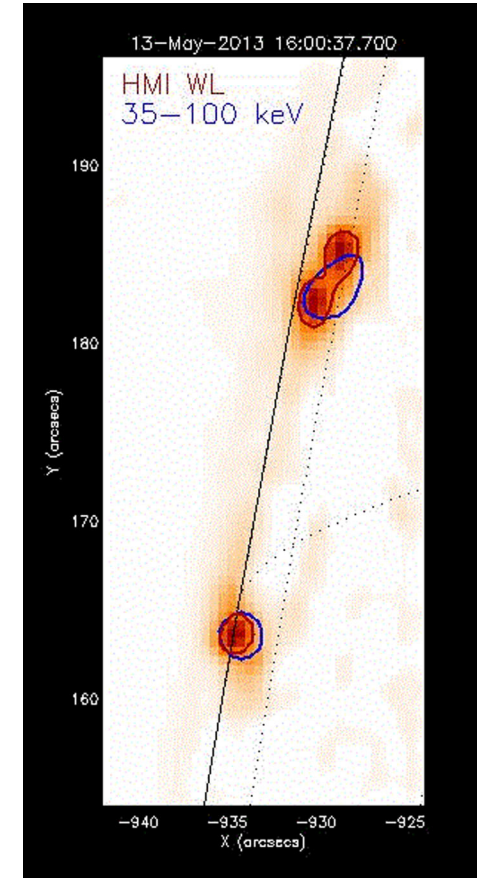
Continuum emission during flares

Bastille day flare: 14 July 2000



Continuum emission during flares

- ❖ WL flare emission correlates in **time** with hard X-rays (Matthews et al. 2003; Metcalf et al. 2003; Hudson et al. 2006).
- ❖ It also coincides in **space** within less than an arcsecond (Krucker et al. 2011).
- ❖ The source region of the WL emission is in the low chromosphere (Krucker et al. 2011; Martínez Oliveros et al. 2012).
- ❖ Recently, the WL emission has been correlated with enhancements in the FUV and NUV passbands.



WL flare near the solar limb.
RHESSI HXR (30-50 keV, blue) contours are overlaid on a WL difference image (HMI/SDO).



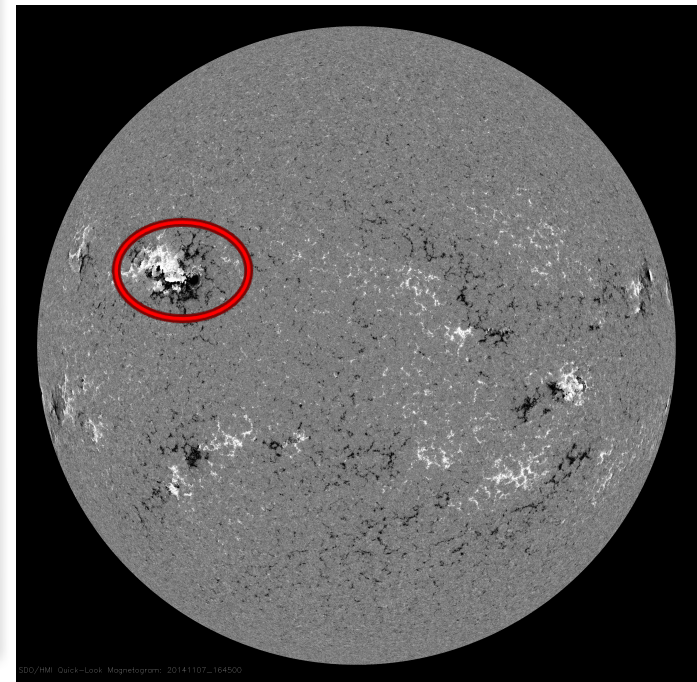
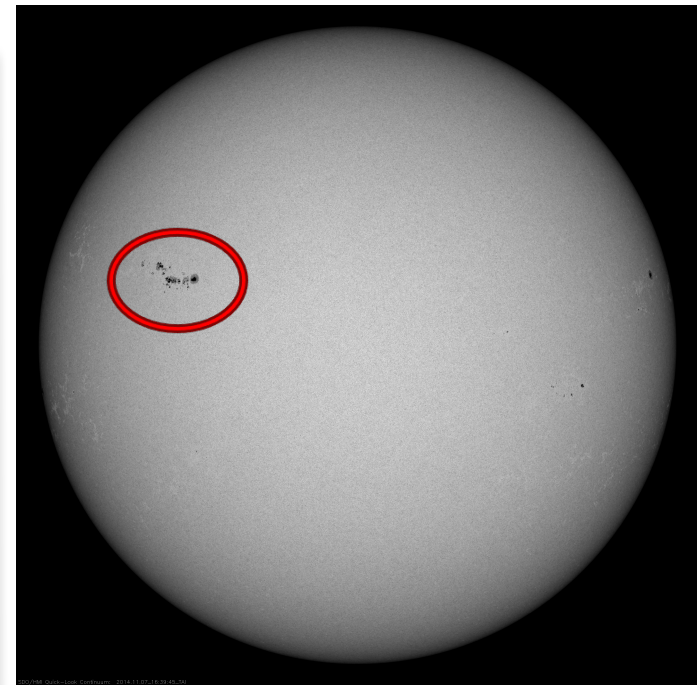
SOL20141107

- Coordinated Observing Campaign
“Searching for signatures
of WL flares”
ROSA & IRIS
(+) SDO & HINODE

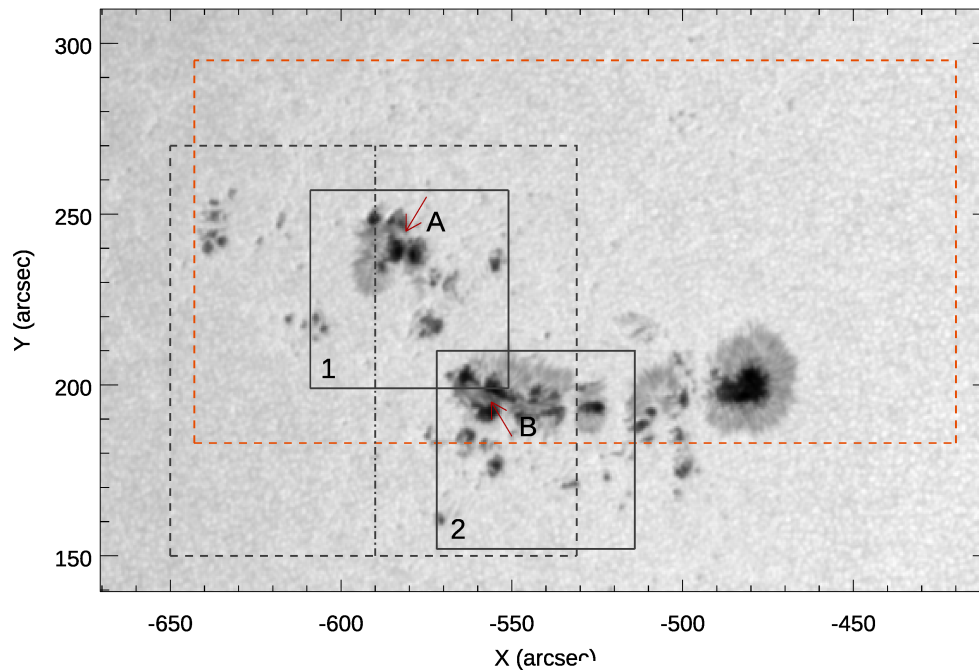
Location: N13E35 (AR 12205)

**A C7.0 flare started at 16:10 UT,
with peak at 16:39 UT**

**An X1.6 flare started at 16:53 UT,
with peak at 17:26 UT**



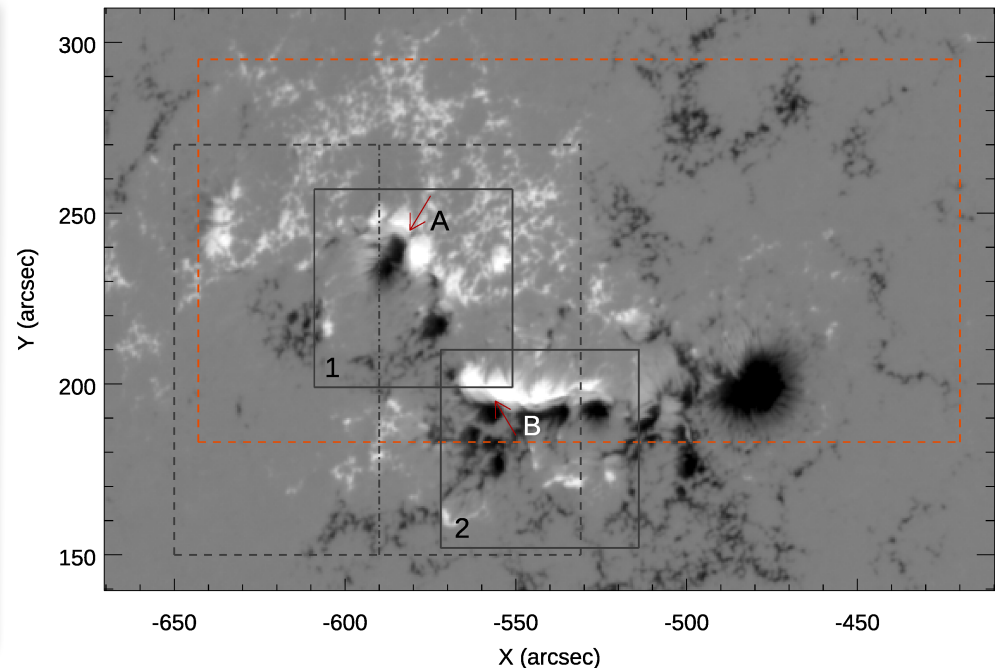
SDO/HMI Continuum 7-Nov-2014 16:58:12.9 UT



Field of view of the different instruments:

- Dashed box: IRIS SJI FOV
- Dotted-dashed vertical line: IRIS slit
- Solid box: ROSA FOVs (1 & 2)
- Red dashed box: Hinode/SOT FOV.

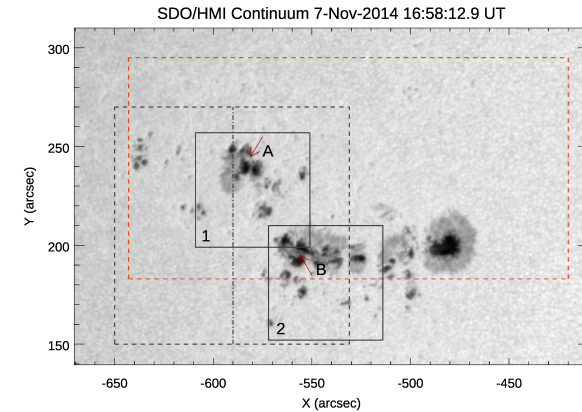
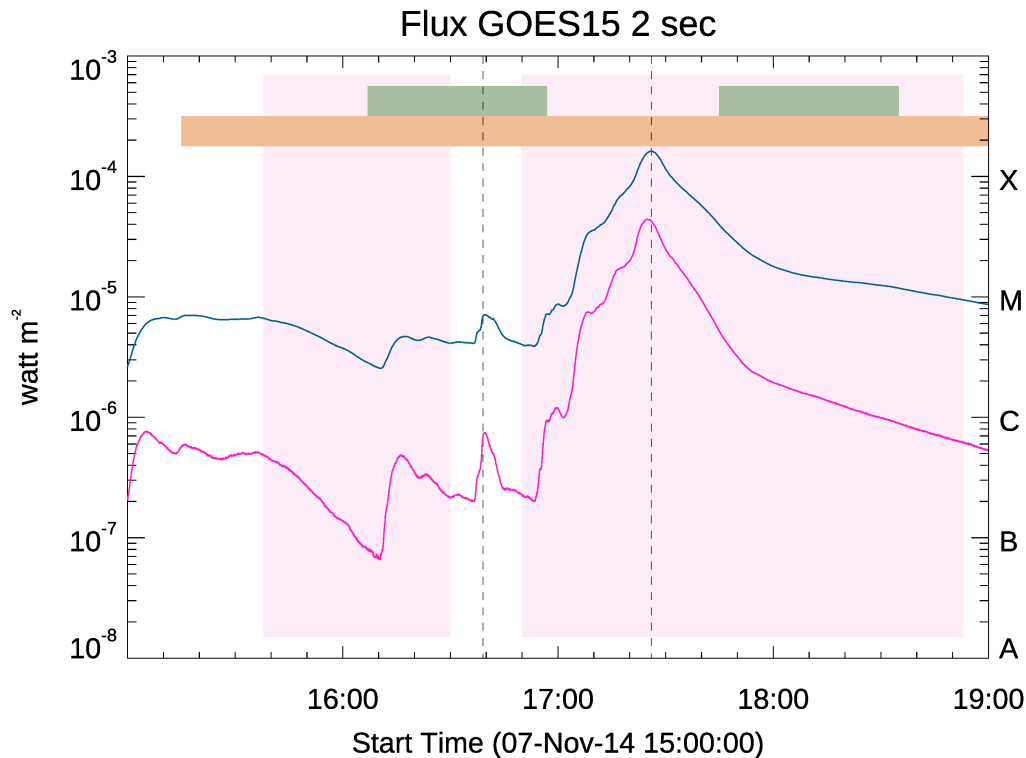
SDO/HMI Magnetogram 7-Nov-2014 16:58:12.9 UT



The arrows indicate the presence of two δ spots (A and B) in both the continuum image (photosphere) and in the magnetogram



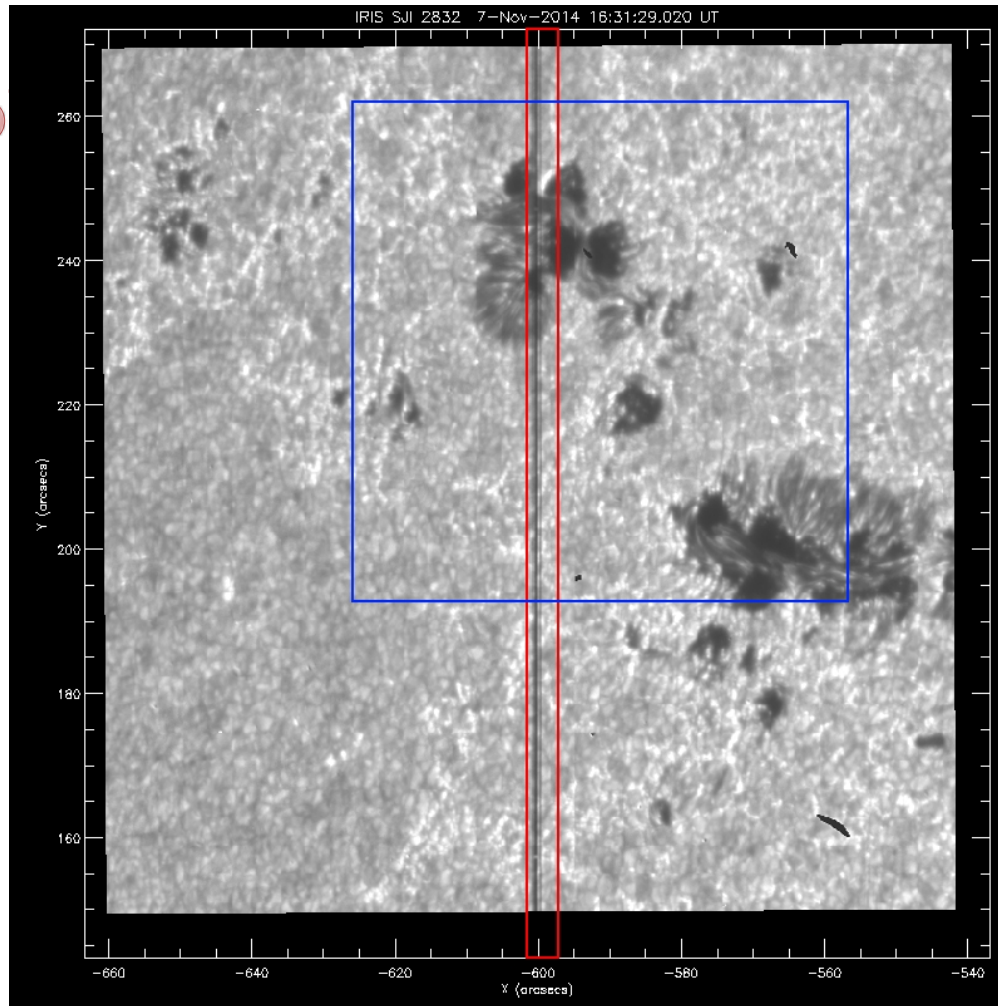
GOES soft X-ray flux and time coverage for different instruments



GOES soft X-ray flux at 0.5 – 4 Å (purple line) and 1.0 – 8.0 Å (blue line).

- ❖ Vertical dashed lines : peak time of the C7.0 (16:39 UT) and X1.6 (17:26 UT) flares
- ❖ Pink rectangles: ROSA acquisition time intervals for FOV1 (left) and FOV2 (right)
- ❖ Green rectangles: IRIS acquisition time intervals
- ❖ Orange rectangle: Hinode/SOT acquisition time interval.

ROSA & IRIS DATASETS



➤ ROSA

- **Ca II K core (3933 Å)**
512x512 0.138 arcsecs/pixel
FOV=70"X70", cadence 2.45 s
- **G band (4305 Å)**
1004x1002 0.069 arcsec/pixel
FOV=70"X70", cadence 2.112 s .

➤ IRIS

- **SJI image**
(**C II 1330 Å, Mg II k 2796 Å ,
Mg II wing 2830 Å**)
760x774 pixels
0.16 arcsec/pixel
FOV=126".43 x128".76
from 16:07 to 16:57 UT
80 images with $\Delta t=37.57$ s
- **Raster (large 4-step coarse)**
(**C II 1336, 1343, Fe XII 1349,
O I 1356, Si IV 1403, 2832, 2826,
Mg II k 2796**)
FOV=6"x128".76
from 16:07 to 16:57 UT
80 images with $\Delta t=37.57$ s
raster step 9.7 s



Queen's University
Belfast

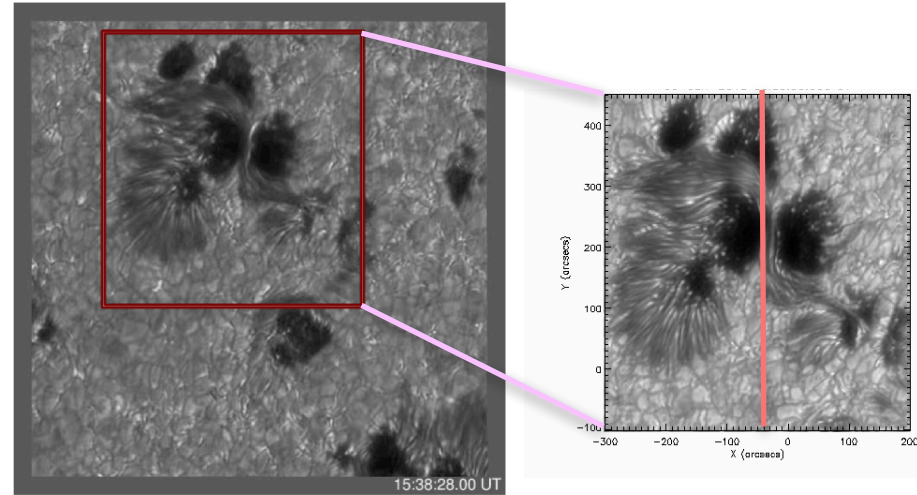


PREEST

ROSA observations

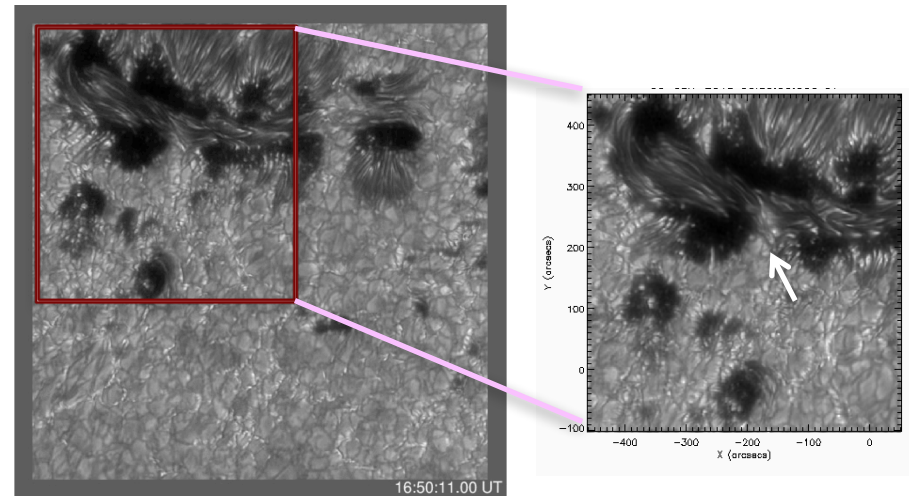
Left: ROSA G band image showing FOV1, before the occurrence of the C7.0 flare.

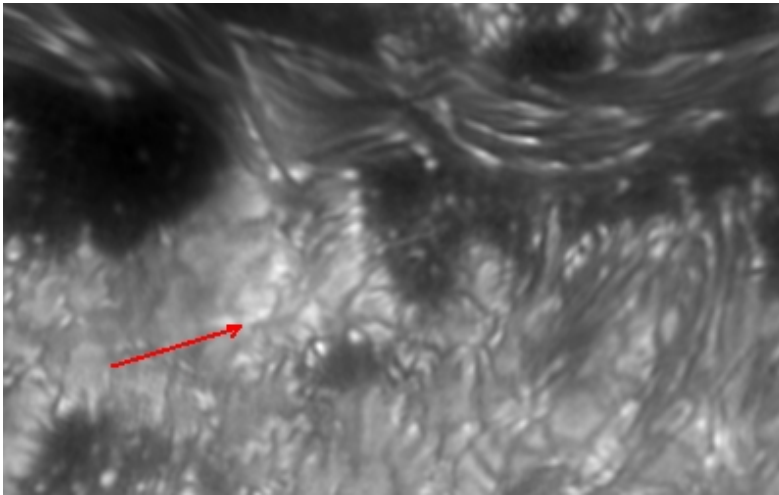
Right: zoomed image showing **δ -spot A**, characterized by the presence of sheared penumbral filaments within the two umbrae of opposite magnetic polarities. The pink vertical line shows the IRIS slit approximate position.



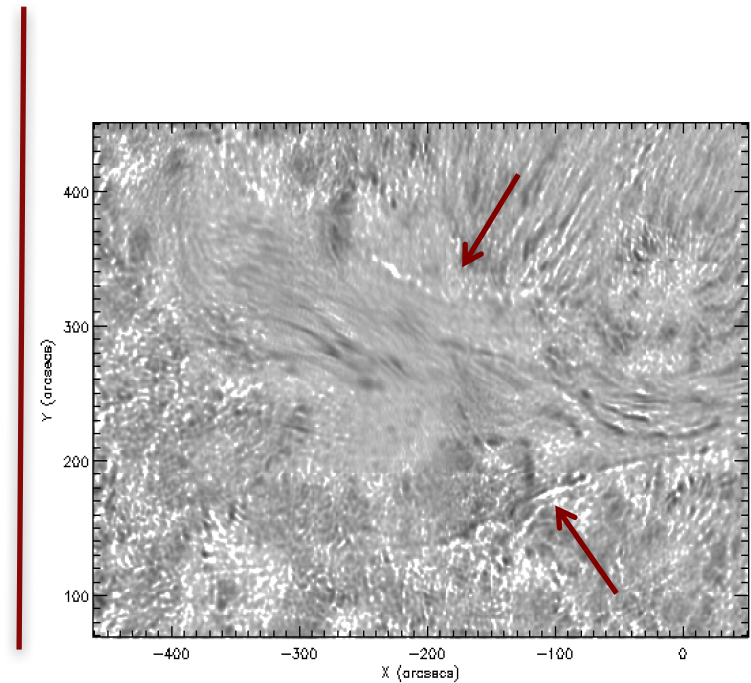
Left: ROSA G band image showing FOV2, during the occurrence of the X1.6 flare.

Right: zoomed image showing the location of a **ribbon observed in the continuum** (white arrow) at about 17:22 UT (i.e., few minutes before the flare peak).





ROSA G band image during the WL flare emission. The red arrow shows the ribbon.



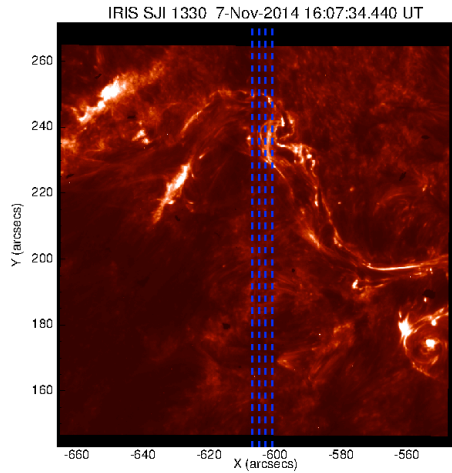
ROSA G band difference image showing part of FOV2, at a time close to the peak of the X1.6 flare.

The dark red arrows indicate the location of the ribbons.

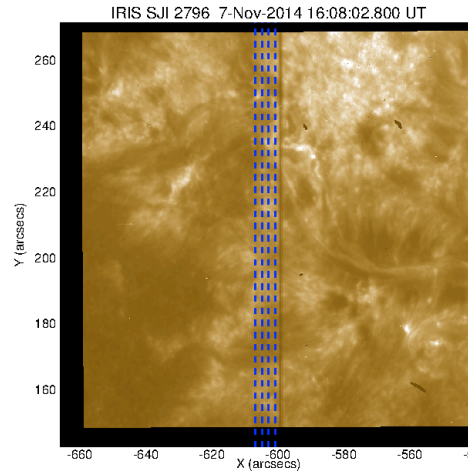


IRIS DATA

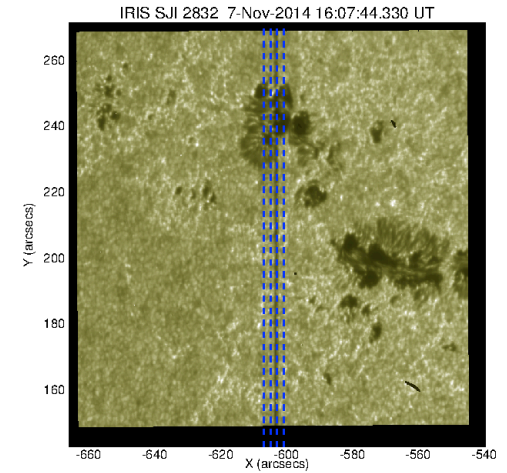
C II 1330 Å 30000 K



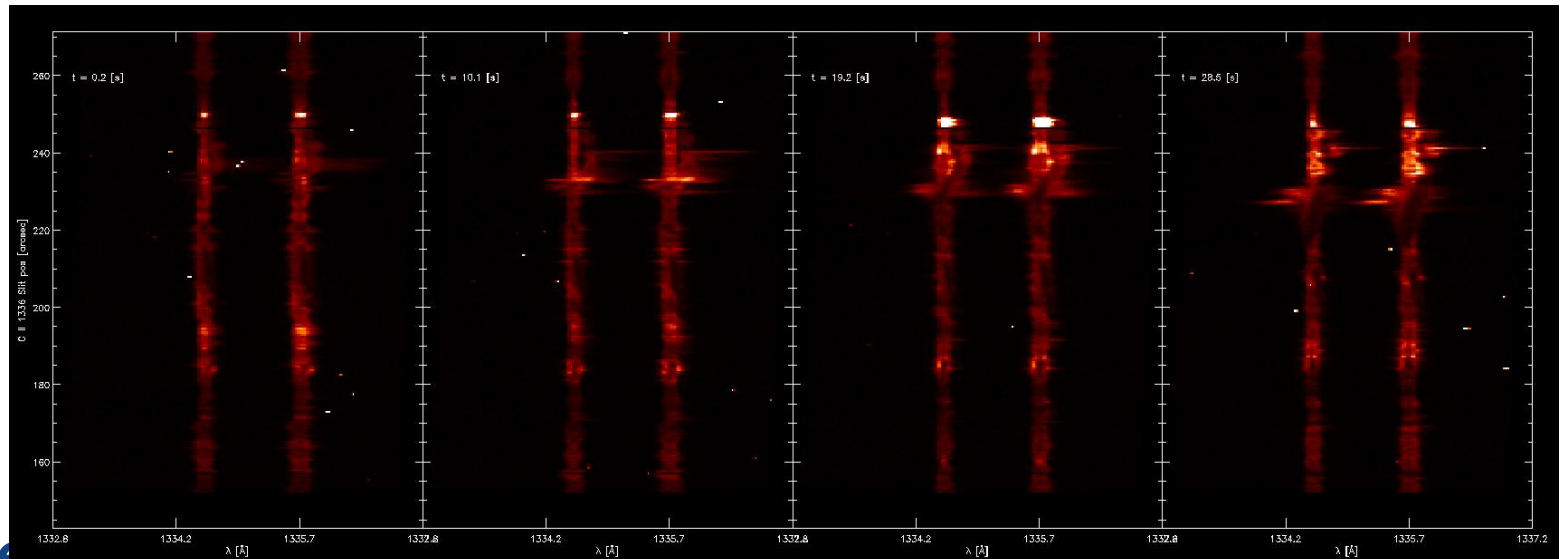
Mg II k 2796 Å 10000 K



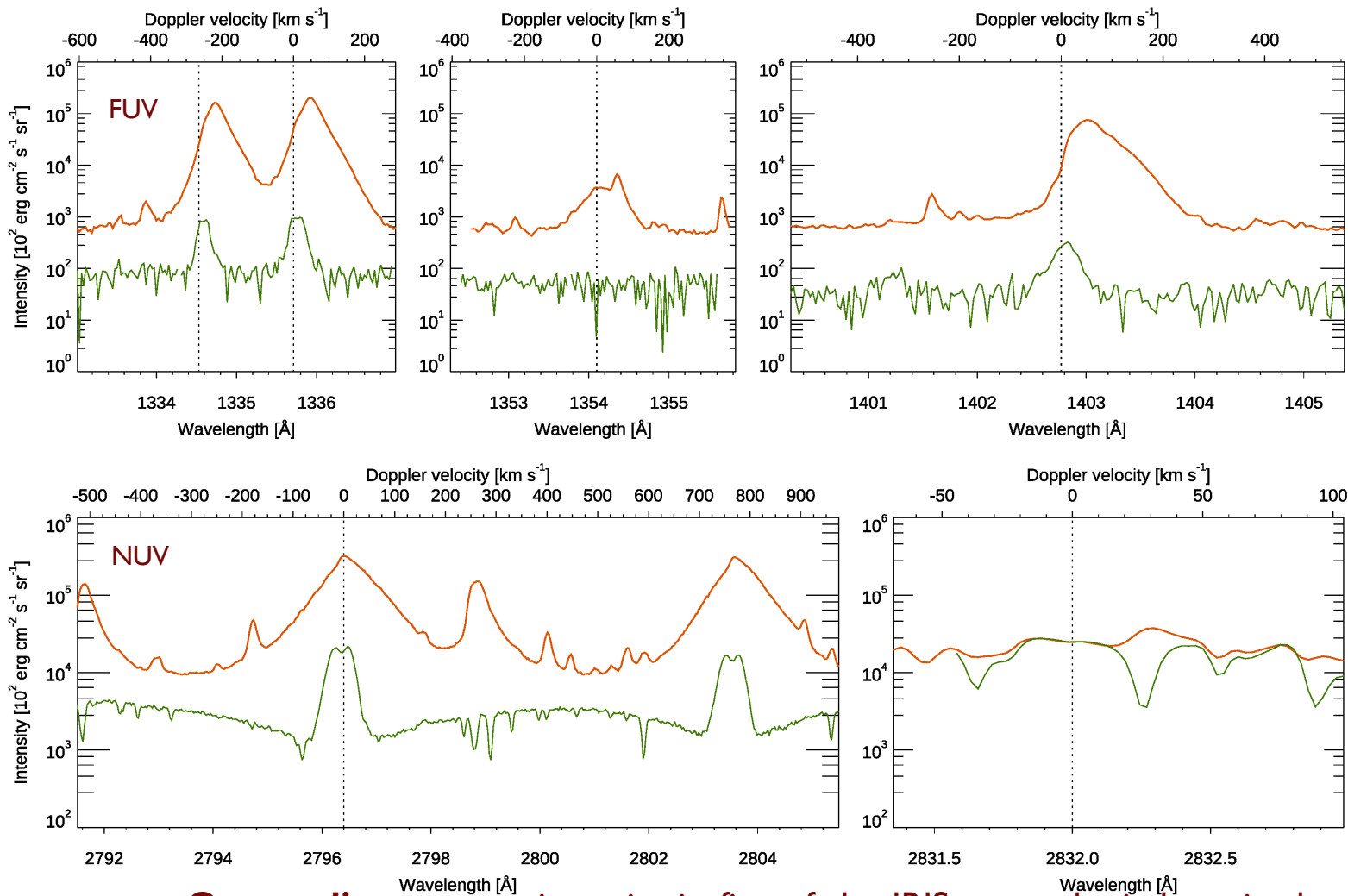
Mg II k wing 2832 Å 6000 K



Raster (1-4) @ C II line, start time 16:07:34 UT, step time 9.7 s



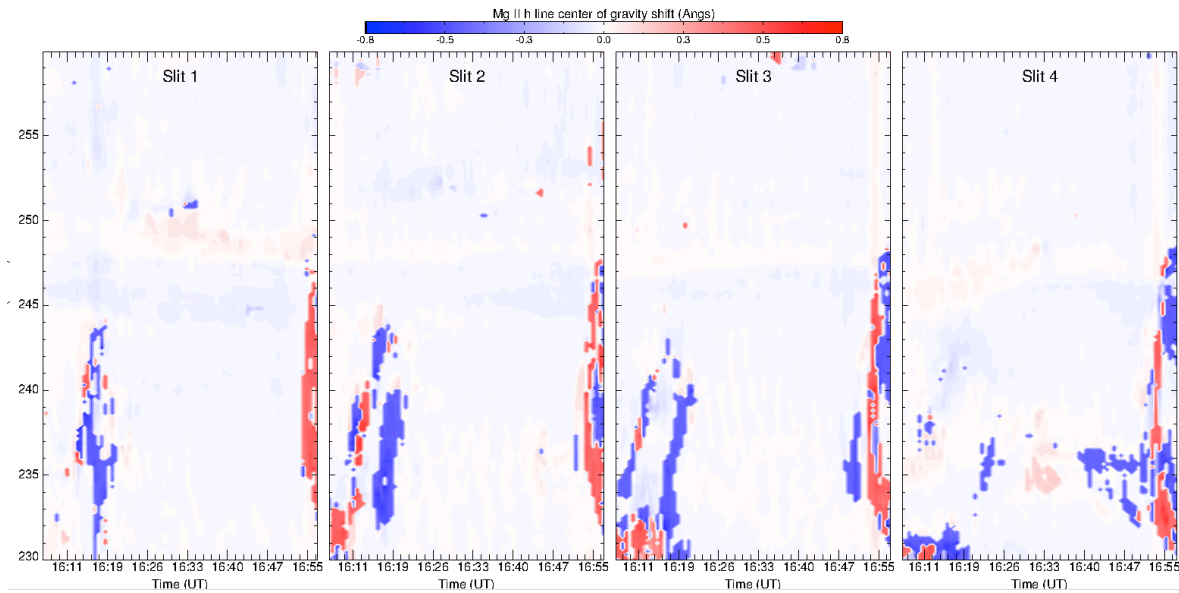
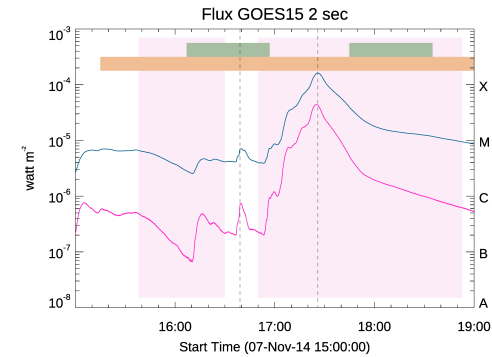
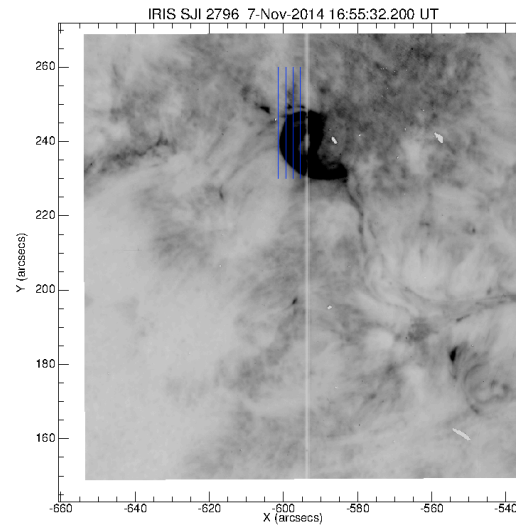
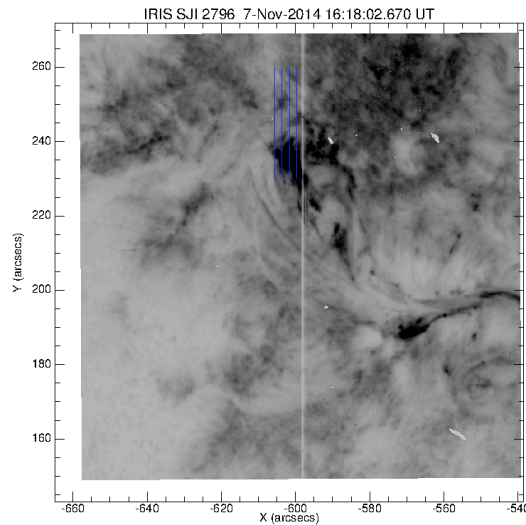
Continuum enhancement in FUV and NUV @ the rise phase of the XI.6 flare



- **Orange line:** average intensity in five of the IRIS spectral windows in the pixels at raster position (3,[558:560]) at 16:55:32 UT
- **Green line:** average intensity calculated at the same time along 20 consecutive slit positions (from I60 to I79), corresponding to a **quiet-Sun region**.



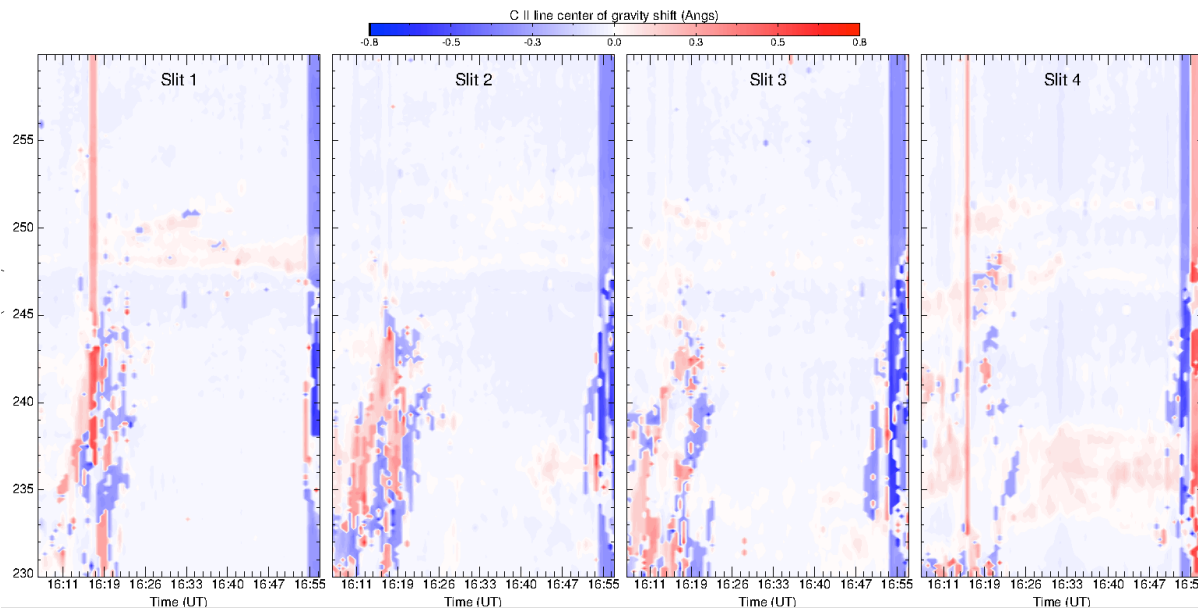
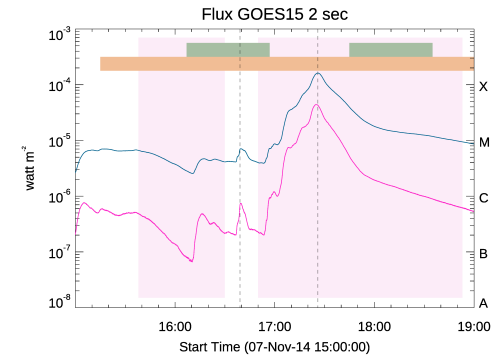
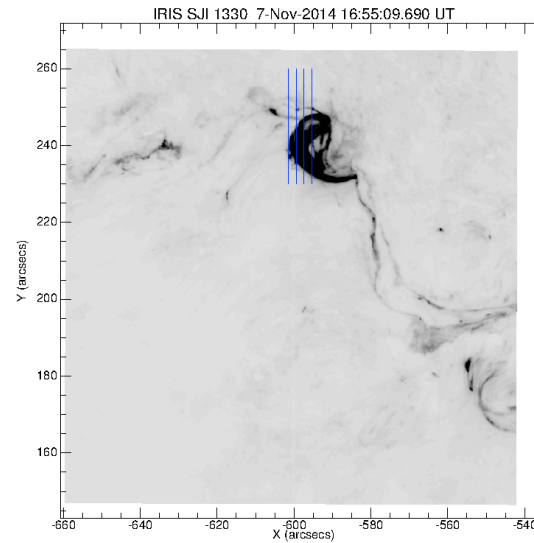
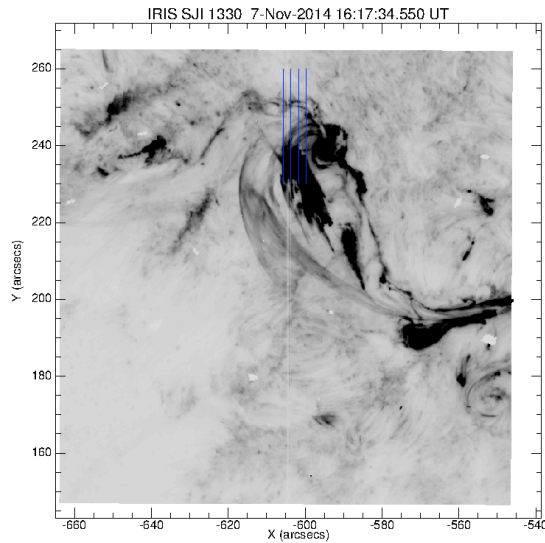
IRIS images at 2796 Å before the peak of the C7.0 flare and during the rise phase of the XI.6 flare

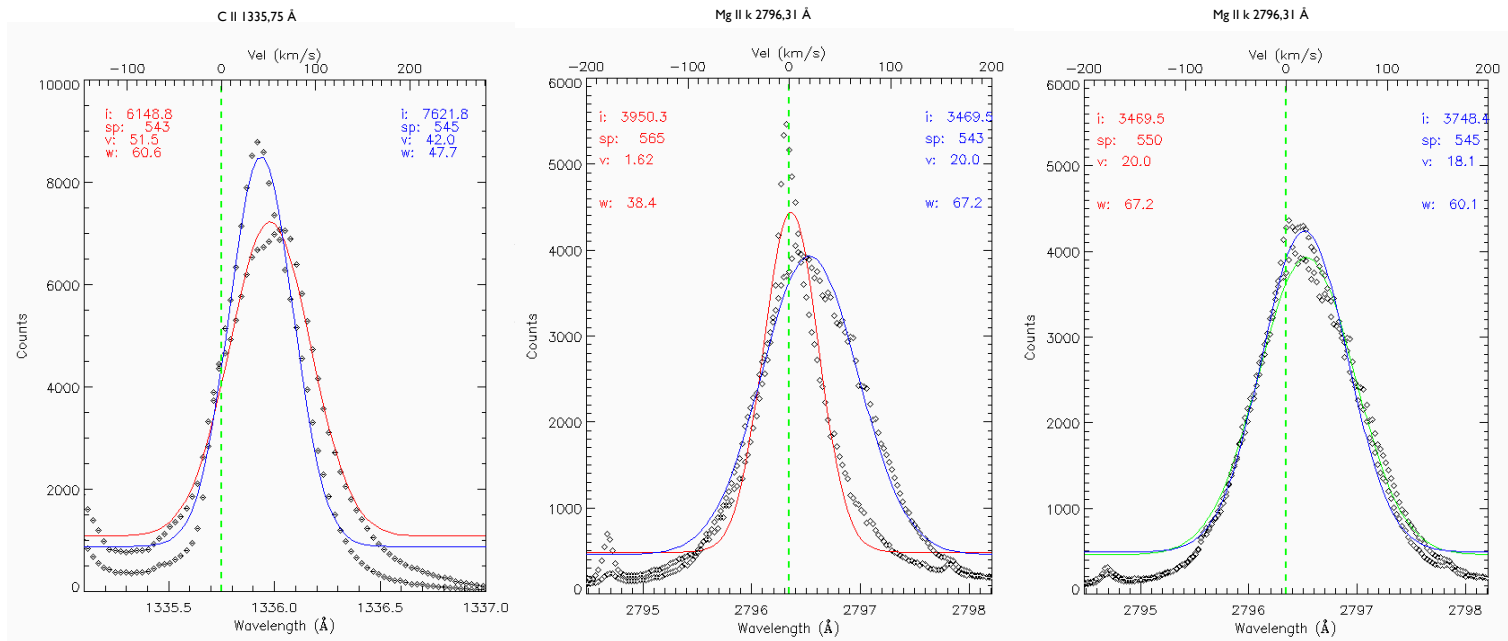


Queen's University Belfast



IRIS images at 1330 Å before the peak of the C7.0 flare and during the rise phase of the XI.6 flare



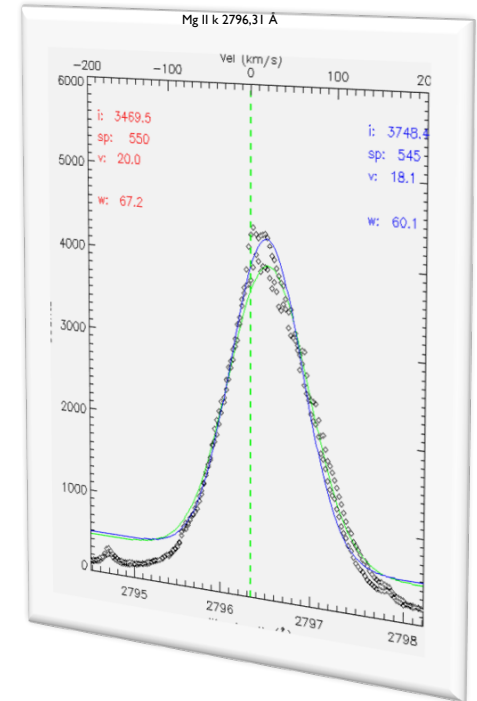
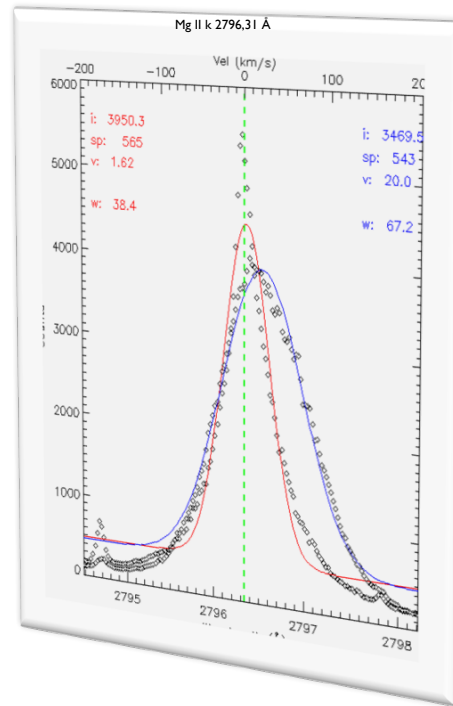
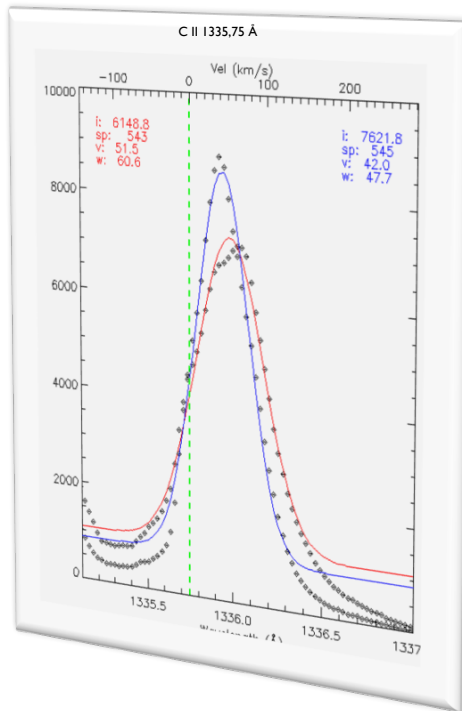


Line profiles for different pixel position of the IRIS slit for C II 1335,75 Å (left panel), Mg II k 2796,31 Å (middle and right panels) at 16:55 UT. The green vertical lines indicate the position of the line center.

In the labels inside each plot the parameter v indicates the plasma velocity deduced from the plots.

Continuous lines indicate the single Gaussian fit and different colors refer to different slit position.



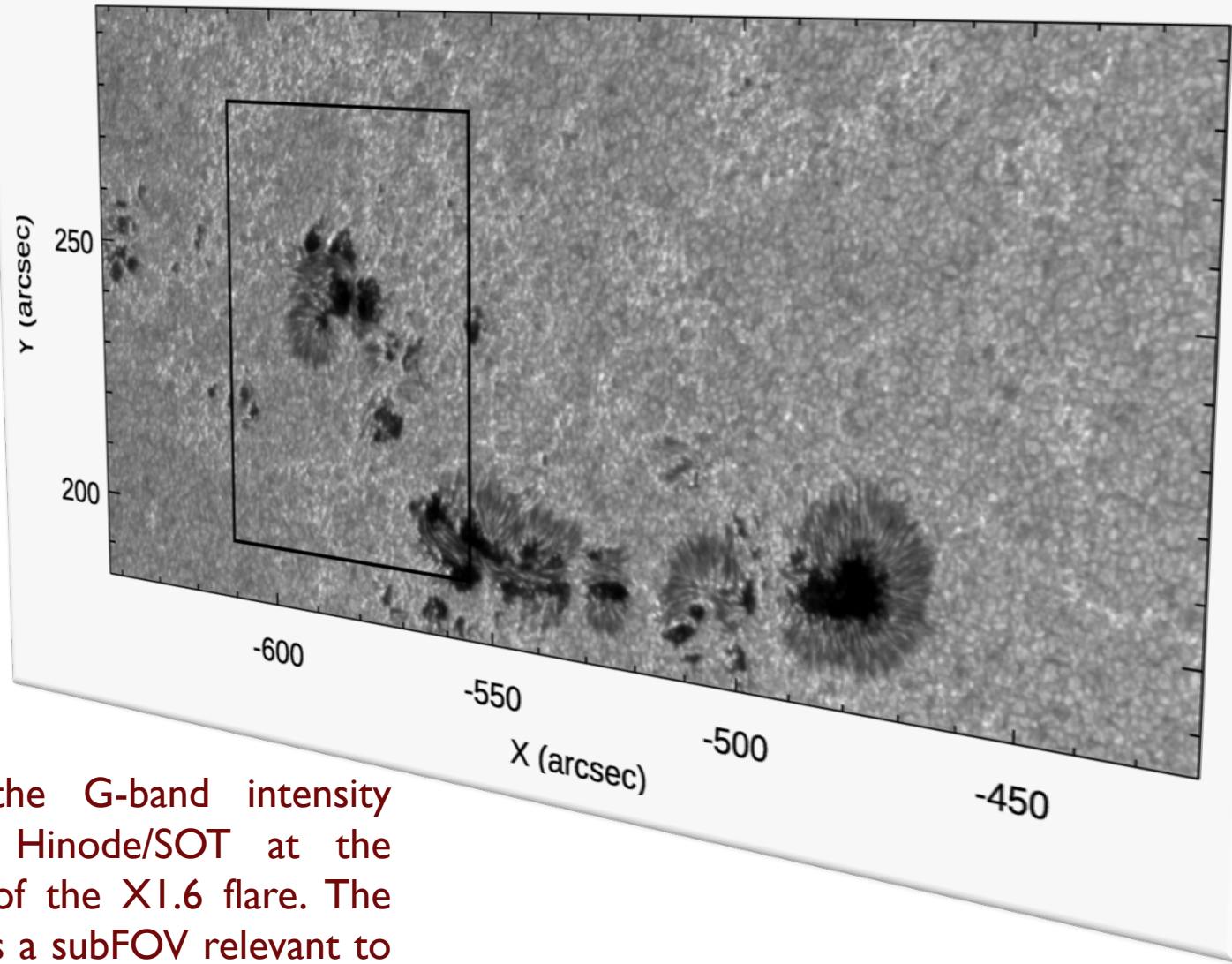


The line profiles and the velocity values indicate that at 16:55 UT there is a **predominance of downward motions**, with velocities in the range **2 - 52 km s⁻¹**.

A process of chromospheric condensation is going on.

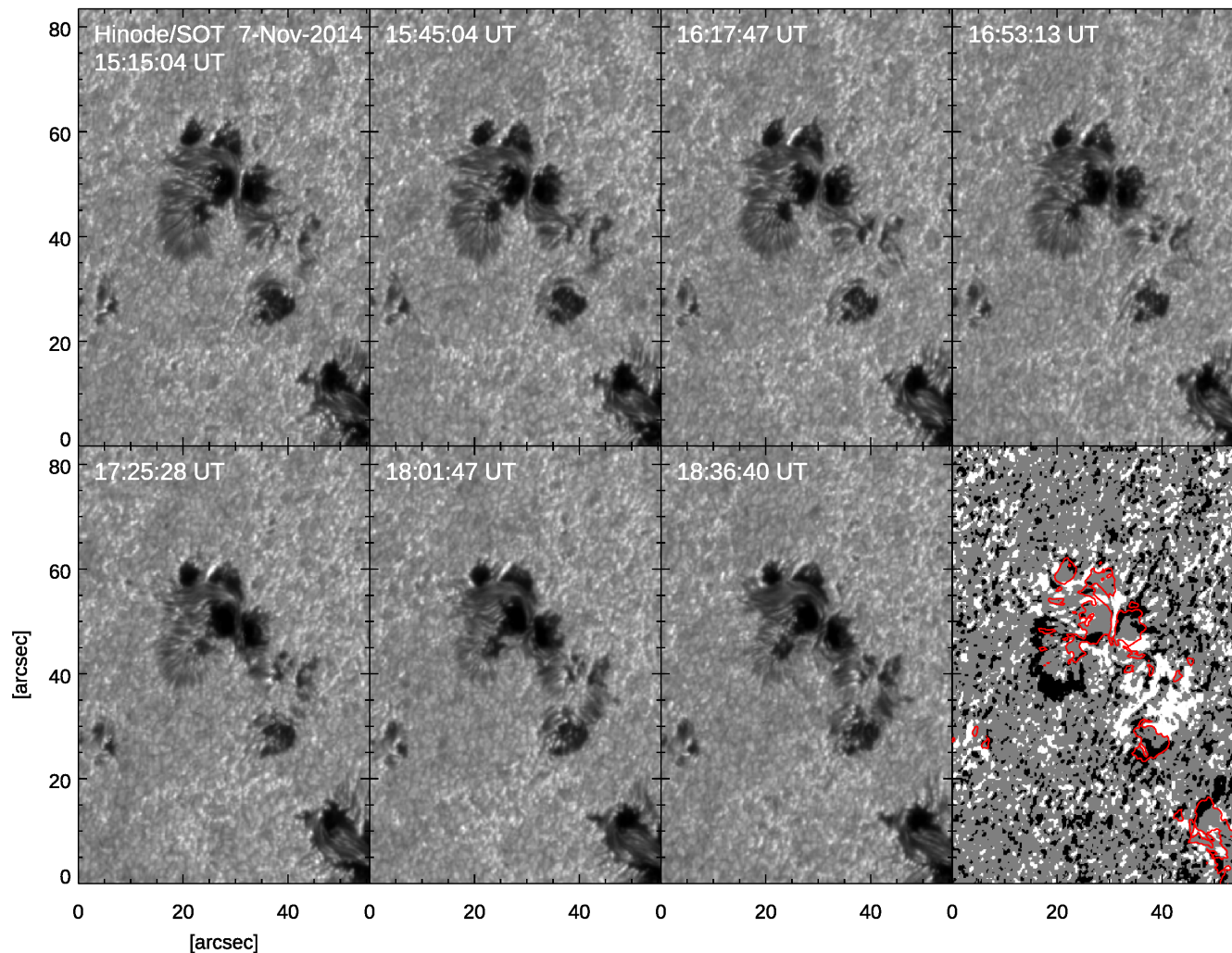


Hinode/SOT 7-Nov-2014 16:53:13 UT



Map of the G-band intensity taken by Hinode/SOT at the beginning of the X1.6 flare. The box frames a subFOV relevant to the A sunspot

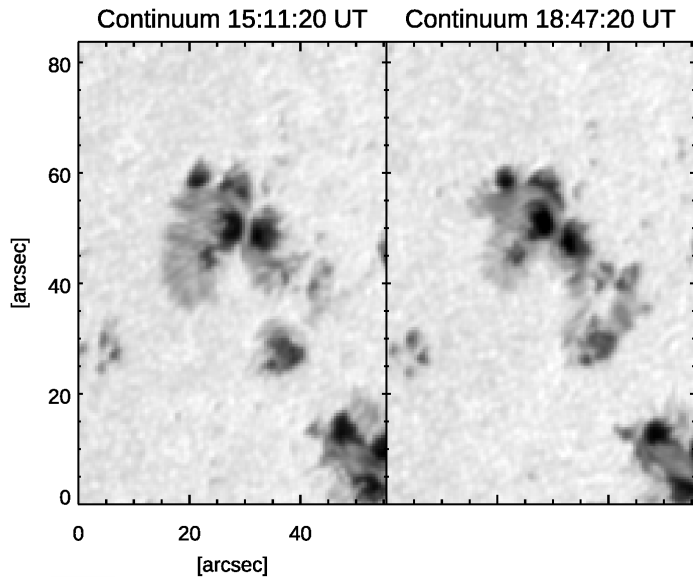




Panels 1–7: Photospheric evolution of the δ complex A during the C7.0 and X1.6 flares, (Hinode/SOT in the G band).

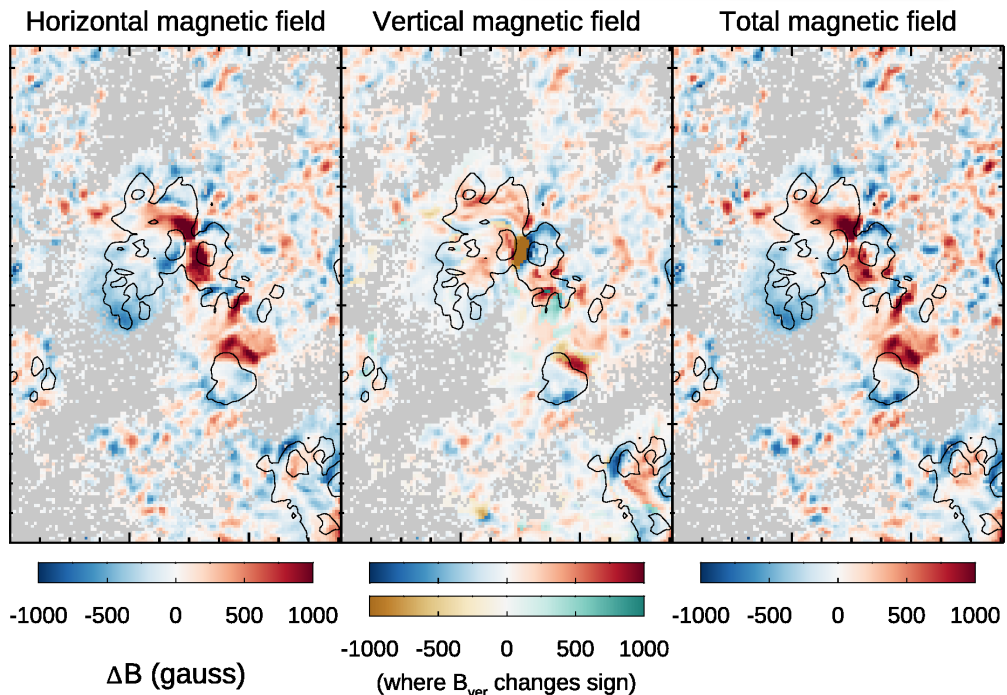
Bottom-right panel: **Difference image between the first and last G-band filtergrams. White (black) areas indicate region with penumbral enhancement (decay).** Red contours indicate the umbral boundary at the beginning of the sequence.

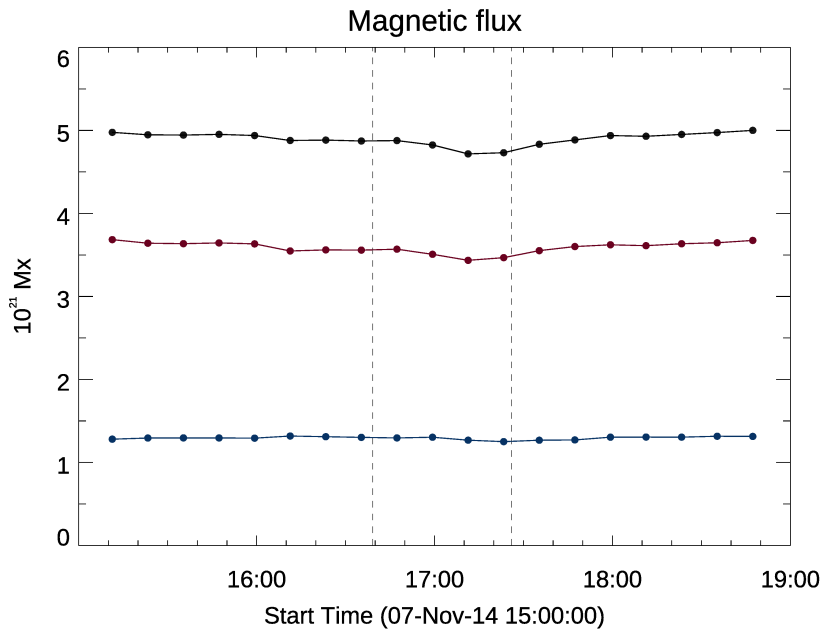




SDO/HMI continuum images of the same subFOV used for Hinode/SOT filtergrams, before (15:11 UT) and after (18:47 UT) the flares.

- Difference images between the final and initial maps of:
- ❖ **horizontal field component**
 - ❖ **vertical field component**
 - ❖ **total magnetic field strength.**





Total unsigned magnetic flux (black), positive flux (red), and negative flux (blue, in absolute value), relevant to the subFOV shown in the previous Figure.

Vertical dashed lines: peak time of the C7.0 (16:39 UT) and X1.6 (17:26 UT) flares.

The changes in the penumbrae are related to magnetic fields becoming more vertical or horizontal, leading to the decay or enhancement of penumbral regions, respectively.

Liu et al. (2005) showed that the flare-associated changes in WL continuum intensity were related with permanent variations in the magnetic field inclination as a result of the reconnection in δ sunspots.



Conclusions

- ❑ During the first flare an enhancement of continuum emission in FUV and NUV, as well as **signatures of emission in the wing of the Mg II k line** were detected, while during the second flare ribbons (**separating at an average velocity of 10 km s^{-1}**) were observed in the **G band** and in the **4170 \AA continuum**.
- ❑ The line profiles of C II $1335,75 \text{ \AA}$ and Mg II k $2936,31 \text{ \AA}$ (IRIS dataset) indicate that at 16:55 UT, there is a **predominance of downward motions**, with velocities ranging between 2 and 52 km s^{-1} , indicating a process of **chromospheric condensation**.
- ❑ Both flares **involved δ sunspots** in the northern and southern parts of the AR. **Changes in the penumbrae** of these sunspots are related to **magnetic fields becoming more vertical or more horizontal**.



Questions (and potential observations) for $\mathcal{E}ST$:

- *What constraints can we single out from the analysis of the photospheric magnetic field and from continuum emission?*
- *Can we shed light on the chromospheric evaporation/condensation process?*



The research leading to these results has received funding from the European Commissions Seventh Framework Programme under the GA no. 606862 (F-CHROMA project) and from the European Union's Horizon 2020 research and innovation programme under GA no. 739500 (PRE-EST project).